

Simultaneous density contrast is bidirectional

Hua-Chun Sun

McGill Vision Research, Department of Ophthalmology,
McGill University, Montreal, Quebec, Canada



Curtis L. Baker Jr.

McGill Vision Research, Department of Ophthalmology,
McGill University, Montreal, Quebec, Canada



Frederick A. A. Kingdom

McGill Vision Research, Department of Ophthalmology,
McGill University, Montreal, Quebec, Canada



Simultaneous density contrast, or SDC, is the phenomenon in which the perceived density of a textured region is altered by a surround of different density (Mackay, 1973). SDC provides an experimental tool to investigate mechanisms of density coding, yet has not been systematically examined. We measured SDC with a 2AFC staircase procedure in which human observers judged which of two patterns, one with and one without a surround, appeared more dense. We used a range of surround densities varying from very sparse to very dense (0–76.8 dots/deg²), and two center test densities (6.4 and 12.8 dots/deg²). Psychometric functions were used to estimate both the points of subjective equality (PSE) and their precision. Unexpectedly we find a bidirectional SDC effect across the five observers: Not only does a denser surround reduce perceived density of the center, but a sparser surround enhances its perceived density. We also show that SDC is not mediated by either contrast-contrast or spatial-frequency contrast. Our results suggest the presence of multiple channels selective for texture density, with lateral inhibitory interactions between them.

Introduction

Textures contain information about surface properties and object boundaries. Textures can vary in many dimensions, including their Fourier spectra (Bergen & Landy, 1991) and higher-order texture statistics (Julesz, 1981; Portilla & Simoncelli, 2000), and the functional roles and neuronal encoding of these different kinds of variations are still only partially understood. One such texture property is the density or numerosity of texture markings, which we will here refer to as texture density. Texture density can have a salient effect on surface appearance, and can be important for the identification and discrimi-

nation of surfaces or objects (e.g., slant and shape from texture; Cutting & Millard, 1984; Todd & Thaler, 2010). Moreover, texture density can affect the ability to segment textures, and changes in it can enable segmentation (Zavitz & Baker, 2013, 2014). In addition, texture density (in our generalized sense of the word) is relevant for mediating numerosity judgements, since number = density × area (e.g., Dakin, Tibber, Greenwood, Kingdom, & Morgan, 2011; Morgan, Raphael, Tibber, & Dakin, 2014; Raphael & Morgan, 2015; Tibber, Greenwood, & Dakin, 2012). Texture density is a separately adaptable feature, suggesting that there exist neuronal mechanisms for its encoding (Durgin, 1995, 2001; Durgin & Hammer, 2001; Durgin & Huk, 1997; Durgin & Proffitt, 1996).

Most studies that have investigated texture density (henceforth “density”) have employed adaptation (Durgin, 1995, 1996; Durgin & Proffitt, 1991, 1996), and some of these studies have demonstrated that density coding is distinct from contrast and spatial frequency coding (Durgin, 2001; Durgin & Hammer, 2001; Durgin & Huk, 1997). These studies have also suggested that adaptation only ever reduces perceived density: Denser adaptors reduce perceived density, yet sparser adaptors have not been found to enhance perceived density. In other words the density aftereffect is apparently unidirectional, implying that density information is coded as a scalar, as with contrast (Durgin & Huk, 1997). However, the aforementioned studies have only investigated a limited range of adaptor densities, and do not rule out the possibility that the density aftereffect might be bidirectional, i.e., that adaptation could both increase as well as decrease perceived density.

An alternative approach for studying how visual attributes are encoded is to investigate spatial as opposed to temporal contrast, specifically how the

Citation: Sun, H.-C., Baker, C. L., & Kingdom, F. A. A. (2016). Simultaneous density contrast is bidirectional. *Journal of Vision*, 16(14):4, 1–11, doi:10.1167/16.14.4.



perception of a visual attribute is altered by a surround with a different level of that dimension. Such “simultaneous contrast” effects have been demonstrated, for example, with luminance (Heinemann, 1955), contrast (Chubb, Sperling, & Solomon, 1989; Georgeson, 1985), spatial frequency (Klein, Stromeyer, & Ganz, 1974), orientation (Blakemore, Carpenter, & Georgeson, 1970; Clifford, 2014), and object size (Roberts, Harris, & Yates, 2005). Mackay (1973) reported an effect of simultaneous density contrast, or SDC, in noise texture patterns, but his study unfortunately conflated density with spatial frequency. More recently Durgin and Proffitt (1991) provided a demonstration of SDC using dot textures (see demonstration in Figure 1A). However, to our knowledge there have been no quantitative measurements of SDC, particularly with a systematic manipulation of center and surround densities. In this study we aimed to further our understanding of density processing by using a 2AFC task to measure SDC as a function of the relative densities of center and surround. We present dot textures in a center–surround configuration and measure the perceived density of the central region while varying surround densities over a wide range, from very sparse to highly dense. We were particularly interested to see if SDC is separable from contrast and spatial-frequency contrast effects, and to determine whether it is coded as a scalar property, as suggested previously.

Materials and methods

Apparatus and stimuli

Stimuli were presented on a CRT monitor (Sony Trinitron GDM-F520, 20 inch, 1600×1200 pixels, 85 Hz, Sony Corp., Tokyo, Japan) at a viewing distance of 57 cm. Luminance was measured with an Optikon universal photometer (Optikon Corp. Ltd., Ontario, Canada), and linearized using Mcalibrator2 (Ban & Yamamoto, 2013). Stimuli were generated and presented using custom code in Matlab with the Psychophysics Toolbox (Brainard, 1997; Kleiner, Brainard, & Pelli, 2007; Pelli, 1997). Stimulus textures consisted of quasi-randomly placed dots (0.12°), with a constraint on dot placements to prevent overlap. This was achieved by setting the minimum interdot distance to be negatively proportional to density, specifically equal to $1.68 \times (\text{density} \times 0.167)^{-0.5}$. This holds constant what Durgin (1995) refers to as the “ratio of regularity” (RoR), preventing the occurrence in the relatively sparse displays of dot clusters and blank areas that might influence SDC.

Half of the dots were black (7 cd/m^2) and the remainder white (115 cd/m^2), all on a mid-gray

background (61 cd/m^2), giving a Michelson contrast of 88.5%. Each dot texture pattern was presented in a circular center–surround arrangement, such that the diameter of the center area was 4.35° , and the surround diameter was six times larger (26.09°).

Two kinds of stimuli were presented in successive temporal intervals of each trial: a match and a test. The match covered the center area only, whereas the test contained textures covering both center and surround areas. A set of many possible match stimuli was generated and stored prior to the experiments, ranging across 140 logarithmically spaced density levels, from very sparse (0.13 dots/deg^2) to very dense (51.2 dots/deg^2). The match stimulus for each trial was selected from the 140 levels based on a staircase procedure. The center of the test stimulus was set at either of two density levels (6.4 dots/deg^2 and 12.8 dots/deg^2), and at one of eight relative surround density levels: test center density $\times 0$ (“no-surround” baseline), $1/216$, $1/36$, $1/6$, 1 , 2 , 4 , or 6 , i.e., a total of 16 possible density levels for the surround. The absolute densities for the surround conditions were 0 , 0.03 , 0.18 , 1.07 , 6.4 , 12.8 , 25.6 and 38.4 dots/deg^2 , for the test center density of 6.4 dots/deg^2 . For the test center density of 12.8 dots/deg^2 , the densities of the surrounds were 0 , 0.06 , 0.36 , 2.13 , 12.8 , 25.6 , 51.2 , and 76.8 dots/deg^2 . Examples of test stimuli, all with a center density of 6.4 dots/deg^2 , are depicted in Figure 1 for three conditions, having a relative surround density $\times 1/6$ that of the center (Figure 1B), a relative surround density $\times 4$ that of the center (Figure 1C), and a blank surround (“ $\times 0$,” Figure 1D).

Note that there are different ways to define contrast. Michelson contrast is defined by the maximum and minimum luminances, i.e., $(L_{\text{max}} - L_{\text{min}}) / (L_{\text{max}} + L_{\text{min}})$; RMS contrast by pixelwise root-mean-square values. Here we used Michelson contrast to describe the luminance difference between the black and white dots (peak-to-peak contrast), which was kept constant (88.5%) across density levels in the main conditions described already. However, changes in density will result in corresponding changes in RMS texture contrast. To test for the confounding effects of RMS contrast, we used the highest relative surround density level (i.e., $\times 6$) of the two test center densities to create, for each, four logarithmically spaced Michelson contrast levels (5.53%, 11.06%, 22.13%, 44.25%), which corresponded to the RMS contrasts of the four relative density levels of 0.02 , 0.09 , 0.37 , and 1.49 . Together with the original relative surround $\times 0$ density condition (i.e., 0% Michelson contrast) and $\times 6$ density condition (which has 88.5% Michelson contrast as with all the other main conditions), there were six levels of Michelson contrast in total. Altogether our experiment consisted of 8 relative surround densities + 4 additional contrast levels, all at two test center densities, 24 conditions in total.

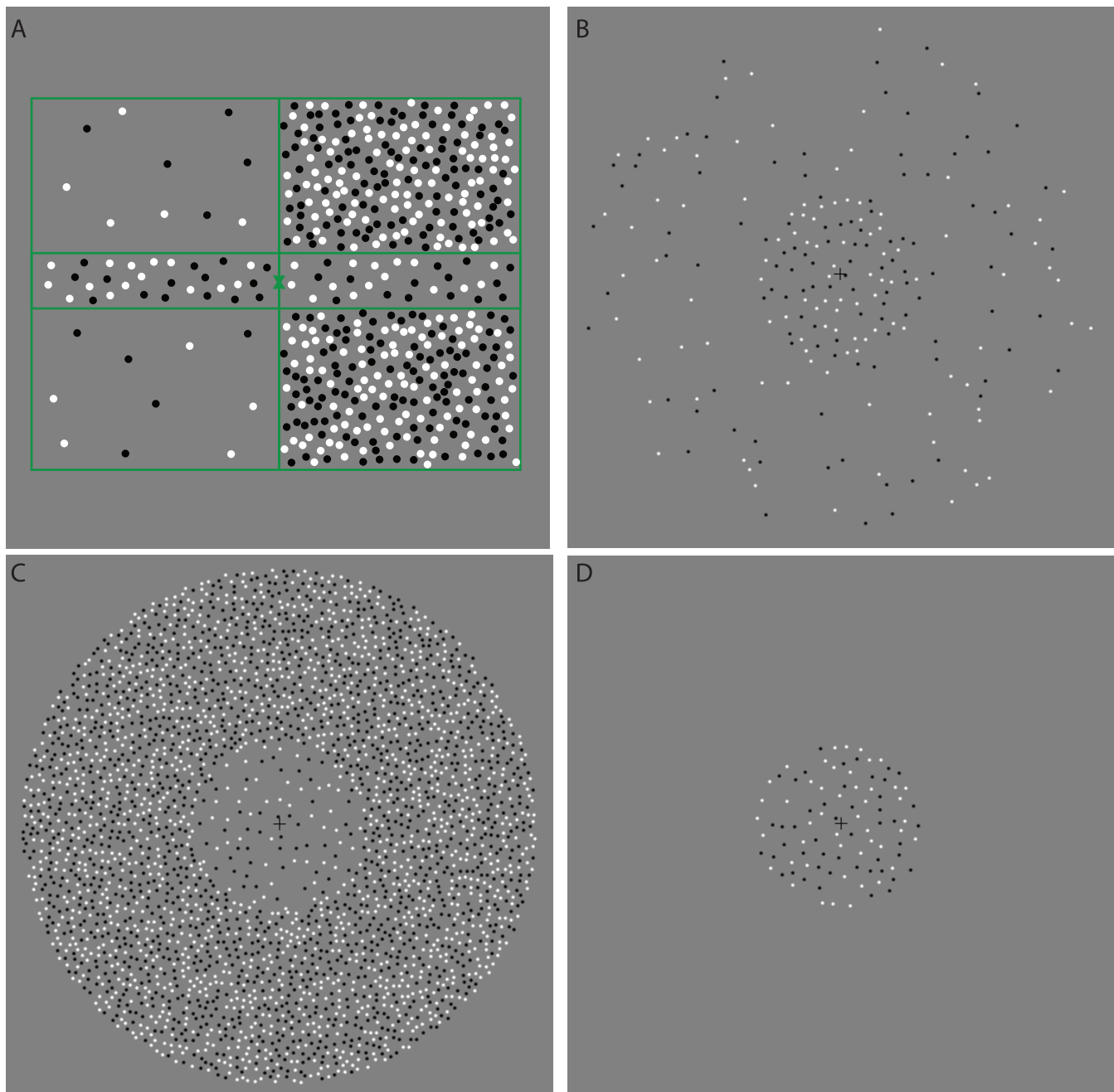


Figure 1. Stimuli to elicit simultaneous density contrast (SDC). (A) Simple demonstration of the SDC. When fixating at the center, the sparser top and bottom patterns on the left side make the middle dot texture appear more dense, whereas the denser top and bottom patterns on the right side make it appear less dense, even though it has the same texture pattern and physical density on both sides. (B–D) Examples of stimuli used in the experiment. The center dot texture in B appears more dense than in D, and the center texture in C appears more sparse than in D, even though all of the center textures have the same physical density. The surround density in B is $1/6$ that of the center, whereas the surround density in C is four times that of the center. Note that in the formal experiment, the diameter of the surround region is six times that of the center rather than two times as shown here.

Design and procedure

The three authors (HCS, CB, & FK) and two naïve volunteers (VL and YJK) participated in observing, all of whom had normal or adjusted-to-normal vision. Each participant completed six sets, in each of which

the 24 conditions were randomly assigned to six trial blocks (four conditions in each block). Each block contained separate interleaved staircases (25 trials each), one for each of the four conditions. In total, there were 150 trials (six independent staircases) for each condition.

In each trial, participants viewed two stimuli in sequence, first a match stimulus and then a test stimulus, each presented for 500 ms and separated by a 750 ms interstimulus interval (ISI). We presented the test stimulus last to avoid potential adaptation effects from the surround. Participants pressed buttons on a numeric keypad to indicate which stimulus appeared to have a center region that was more dense. In practice trials, both the test stimulus and the match were presented with a red circle to define the center area, but this was not shown in the formal experiment. Participants were instructed to respond only to the perceived density of the center areas, regardless of the surround. No feedback was provided since here we are interested in the perceptual appearance (and its bias) not accuracy (though we are interested in the precision of the judgments). Participants had unlimited time to make a response, with the next trial following after a 1 s interval. A fixation cross (0.34° in width) was always presented in the center of the screen, to avoid misalignment of the retinal images of the center areas between the test stimulus and the match.

The density level of the test stimulus was specified by the experimental condition while the density level of the match in each trial was adjusted by a staircase procedure, independently conducted for each of the conditions being interleaved within a trial block. We used a staircase with a one up, one down rule, which is well suited for acquiring a point of subjective equality (PSE) in an appearance judgment (Kingdom & Prins, 2016). The density level of the match in the first trial of each staircase was randomly chosen in a range bracketing the predicted PSE level, ± 21 – 25 density levels higher or lower. The predicted PSE level of each participant in each condition was determined based on their pilot data. The jump size (density difference) of subsequent match trials in a staircase was gradually reduced from 22 to two density levels in the first 11 trials, and was kept the same for the last trials for convergence.

Data analysis

Individual data analysis

Trial responses in each condition were first summed across the six staircases for each match density level. We then fitted a logistic psychometric function to each condition using a maximum likelihood criterion, using the Palamedes Toolbox (Prins & Kingdom, 2009). We chose the logistic function because it tends to give robust curve-fits for this type of data. Since the density levels of the match and test stimuli were logarithmically spaced, they were log-transformed before fitting. PSEs were estimated from the fits, which were then transformed back to linear-scale values. Slope estimates were also determined with and without log transfor-

mation for comparison. To estimate standard errors for PSE and slope, we performed a bootstrap analysis (Efron & Tibshirani, 1994) in Palamedes that simulated 400 sets of hypothetical data based on the collected data (Kingdom & Prins, 2016).

Group data analysis

The individual PSE and slope values for the five participants were pooled by taking their geometric means and geometric standard errors.

Data analysis for contrast controls

In order to make the results of the contrast control conditions comparable with those of the main conditions, we transformed the control condition contrasts into equivalent density levels, i.e., density levels with the same RMS contrast. To do this we first measured the RMS contrast for each of the 16 main conditions, and plotted this as a function of density. These functions were well described as power functions, for test center densities of 6.4 and 12.8 dots/deg² condition respectively:

$$RMS = 0.1098D^{(0.5003)}$$

$$RMS = 0.1553D^{(0.4994)}$$

where D = relative surround density.

Using these equations we calculated an equivalent D for each control condition RMS .

Spatial frequency analysis of stimuli

To assess whether spatial frequency components covary with density, we performed an image-processing analysis. We used Log-Gabor filters (Field, 1987) to decompose images of random dot textures of different center density (6.4, 12.8, 25.6, 51.2 dots/deg²) into six frequency bands: low pass (<21 cycles/image), high pass (>171 cycles/image) and four intermediate bands (171, 85, 43, 21 cycles/image), with each band comprising four orientations (0, 45, 90, and 135°). Reconstructed images from these filters were highly similar to the original images, indicating that these filters capture and maintain most of the important texture information. Pixelwise standard deviations were then calculated for the filtered images in each frequency band, which could be compared for various density levels.

Results

Example psychometric functions (PFs) for naive observer VL are shown in Figure 2, for relative

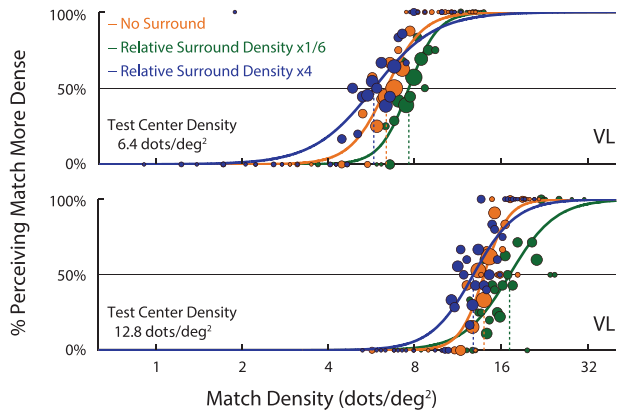


Figure 2. Psychometric functions for naïve observer VL. Each graph plots the proportion of times the match patch appears more dense than the test patch, as a function of match density. Test center densities are 6.4 dots/deg² (top) and 12.8 dots/deg² (bottom), and relative surround densities are ×0 (orange), ×1/6 (green), and ×4 (blue). The diameters of filled circles correspond with the number of trials tested with that value of match density, as determined by the staircase procedure. Continuous lines are best fitting logistic functions. The PSEs are where the vertical dashed lines meet the abscissae and correspond to the 50% horizontal line.

surround densities of ×0, ×1/6, and ×4 and for the two test center densities of 6.4 and 12.8 dots/deg² (upper and lower plots, respectively). Each PF shows the percentage of trials the match density appeared more dense than the test, as a function of the match density. The fitted PSEs are shown as the vertical dashed lines. The size of each data point indicates the relative number of trials at each match density—note that the trials tend to be concentrated around the PSE, as expected given the nature of the staircase procedure. The 12.8 dots/deg² test density PFs (bottom) are shifted to the right of those for 6.4 dots/deg² (top) as expected. Importantly, for both test density conditions, the sparser surround PFs (green) are shifted to the right of, and the denser surround PFs (blue) shifted to the left of, the “no surround” PFs (orange). This indicates that the perceived density of the test appeared greater with a sparser surround and lesser with a denser surround, demonstrating for these PFs a simultaneous density contrast effect that is bidirectional.

The full set of PSEs for the five observers and their group average are shown in Figure 3A and 3B. Each graph shows PSEs as a function of the relative density of the surround (colored) or equivalent contrast (gray). The blue and green lines are for the 6.4 and 12.8 dots/deg² test center conditions, respectively, and are plotted as a function of relative surround density, whereas the gray lines are plotted as a function of equivalent contrast. The horizontal red lines are the PSEs for the “no-surround” baseline conditions—thus points above the red lines imply that the test density appeared more dense, and

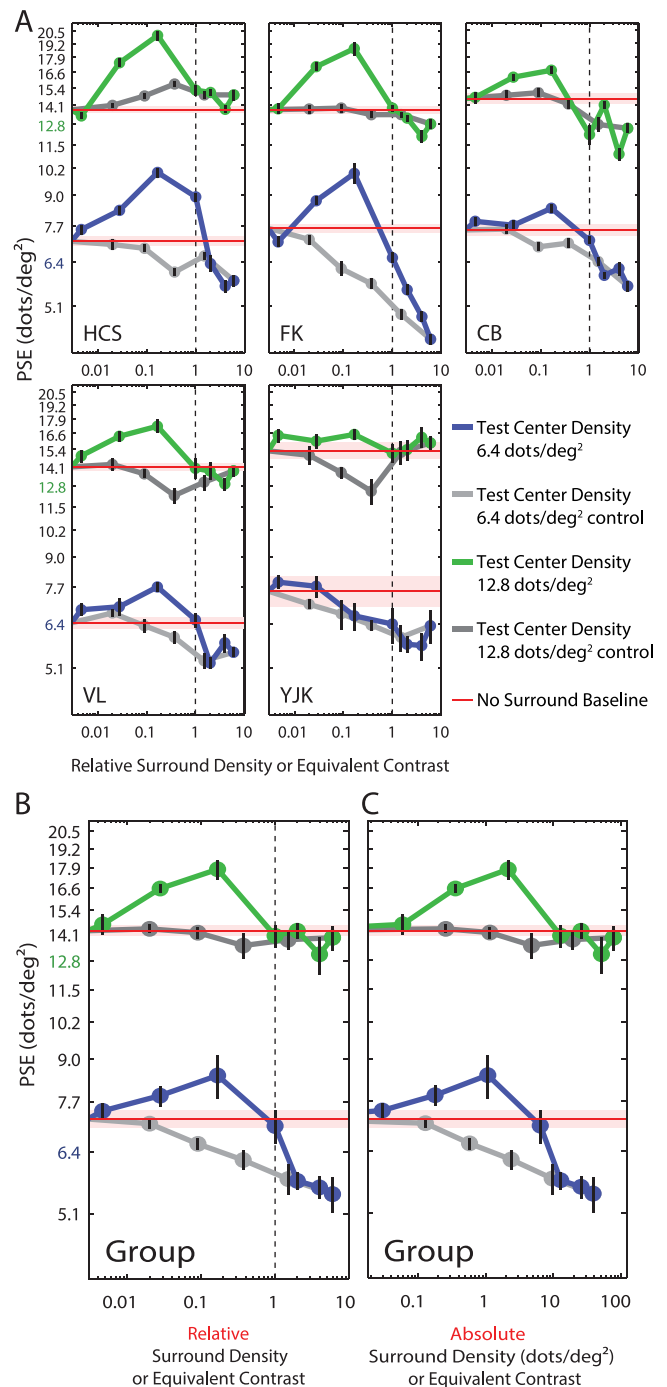


Figure 3. Individual and group PSE results. (A) Graphs showing individual PSE data as a function of the ratio of surround to test density for the five observers, and their group average (B). Blue lines show PSE values for the 6.4 dots/deg² and green lines for the 12.8 dots/deg² test condition. Light gray and dark gray lines depict the equivalent contrast conditions. “No-surround” PSEs are indicated by the horizontal red lines. Error bars (for no-surround conditions the pink areas) are bootstrap-estimated standard errors. Vertical dashed lines represent points where surround and test densities are physically equal. For the group data the geometric mean PSEs and geometric standard errors calculated across subjects are shown. (C) The same group data, plotted as a function of absolute surround density (dots/deg²).

points below the red lines imply that the test density appeared less dense compared to the no-surround conditions. The vertical black dashed lines show the points where match and test densities were physically the same. The patterns of the data are generally consistent across observers in showing a bidirectional effect of surround density. For the denser surrounds there is a smaller PSE shift below baseline for the higher compared with lower test densities. The maximum shifts in perceived density from the sparser surround are on average 17.1% and 24.9% for the 6.4 and 12.8 dots/deg² test conditions, while in the opposite direction the maximum shifts from the denser surrounds are 21.9% and 8.2% for the two test conditions (Figure 3B). This demonstrates that the SDC effect is rather salient for both sparse and dense surrounds (except for the denser surrounds with the 12.8 dots/deg² test conditions, where the SDC effect might have become saturated).

The equivalent contrast PSEs (gray lines) show little evidence of a bidirectional response, generally forming relatively straight lines between their endpoints. Note that the fact that the gray lines are not flat is inevitable given that they converge with the red no-surround baselines on the left of the graph (the no-surround baselines equal 0% Michelson contrast conditions), and the green or blue lines on the right, where the contrast control and main-experiment conditions are identical (the relative surround density of $\times 6$ equals 88.5% Michelson contrast).

The group data as a function of absolute surround density (dots/deg²) are shown in Figure 3C, for comparison with other studies (see Discussion). The two graphs also show that the peaks and the transition points (intersections with red line) of the green and blue lines are aligned with relative surround density (Figure 3B), not absolute surround density (Figure 3C). This result suggests that changes in the perceived density of the test center are governed by center-surround differences in density.

The precision of the density judgments can be inferred from the PF slopes. Figure 4A shows example PFs for the two test densities, plotted against a logarithmic abscissa (left, as in our primary data analysis) and a linear abscissa (right). The right-hand linear plot reveals that the PF is less steep, and hence less precise, for the higher test density. Group slope data were obtained by averaging across the five observers for all conditions, in linear units. No systematic changes between slope and relative surround densities as well as with the equivalent contrast conditions were found. The average linear-unit slopes for the two test densities and for the various surround conditions are shown in Figure 4B. The left-most bars (no-surround) show that a doubling of test density results in a ~ 1.5 -fold decrease in slope, which is close to a $\sqrt{2}$ relationship between density and precision. For the surround-present conditions the decrease in slope

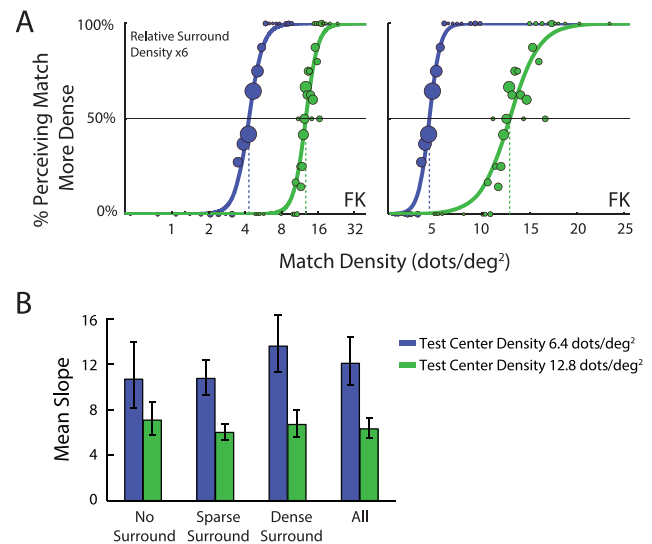


Figure 4. Slope analysis results. (A) Example psychometric functions (left) with and (right) without logarithmically transforming the match densities on the abscissae, for test densities 6.4 (blue) and 12.8 (green) dots/deg² (observer FK, relative surround density $\times 6$ condition). The slope difference between low and high density conditions is clear on the linear abscissa. (B) Group slope results averaged across different conditions. For each observer the slope values were averaged across test density, for, from left to right: relative surround density 0 (“no surround”); relative surround densities of 1/216, 1/36, and 1/6 (“sparse surround”); relative surround densities of 2, 4, and 6 (“dense surround”); and all conditions (“all”). Geometric means and geometric standard errors were calculated across observers.

with test density is closer to a factor of 2, i.e., a Weber relationship between density and precision.

Discussion

Using measurements of simultaneous density contrast (SDC) in random dot patterns, we found not only that a denser surround causes a central test region to appear less dense than otherwise, but a sparser surround causes the same region to appear more dense. This bidirectional SDC effect is unexpected given previous reports that the density aftereffect is unidirectional (Durgin & Huk, 1997). We will return to the significance of this finding.

Induction from contrast and or spatial frequency?

The first question that must be addressed is whether the effects reported here are a byproduct of contrast

induction, since an increasing density of dots at a given amplitude will entail an increase in RMS contrast. We assessed the possible contribution of RMS contrast to the SDC by testing with surrounds of a constant density, whose RMS contrasts equaled those that accompanied the changes in the surround densities employed in the main experiment (Figure 3, grey lines). However, we found no evidence of bidirectionality in the contrast surround data and so we can safely conclude that SDC is not caused by contrast induction, in keeping with findings from the density aftereffect (Durgin, 2001; Durgin & Hammer, 2001). Recently Morgan and MacLeod (2014) showed that for the *threshold* detection of spatial differences in density and/or contrast, density and contrast sum linearly, i.e., are “non-orthogonal.” Our results demonstrate that for the coding of suprathreshold differences in density, such nonorthogonality is not observed.

One might suppose that in varying dot density we inadvertently change the local spatial frequency content of the patterns, and that the surround induction effect is occurring for spatial frequency not density (MacKay, 1973). To examine this possibility, we employed a wavelet analysis of the spatial frequency composition of our dot textures for four values of density (Figure 5). Each texture was filtered into six spatial frequency bands using Log-Gabor filters, and the *SD* of pixel values calculated. Figure 5 shows that the dependence of *SD* on spatial frequency band is identical, to within a scale factor, for all the density levels. Other frequency bands beyond the range shown in Figure 5 were also examined. No differential changes in *SD* across frequency band with density were found. Therefore it is hard to see from this result how spatial frequency contrast could mediate SDC, and hence it does not appear to be the basis for the bidirectionality in SDC. Again, this is consistent with evidence from the density aftereffect (Durgin & Huk, 1997).

Bidirectional versus unidirectional effects

Studies of the density aftereffect have suggested that density adaptation acts in a unidirectional manner, i.e., adaptation only ever reduces perceived density, never increases it (Durgin & Huk, 1997; Durgin & Proffitt, 1991). This would be similar to contrast adaptation, which only ever reduces perceived contrast (Georgeson, 1985), consistent with the idea that neuronal responses to contrast are generally monotonic (but see Ledgeway, Zhan, Johnson, Song, & Baker, 2005; Peirce, 2007). However, to our knowledge there has been no systematic examination of the density aftereffect across a wide range of adaptor/test density ratios, so

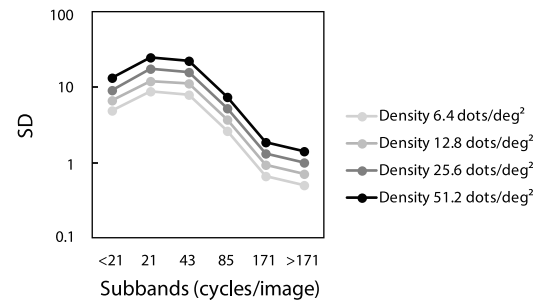


Figure 5. Wavelet analysis of spatial frequency bands in random dot stimuli. The images of the four center density levels indicated were decomposed into six spatial-frequency bands by Log-Gabor filters. Response in each frequency band was estimated as pixelwise *SD* of the filtered images. Density increases the *SD* in all frequency bands similarly.

one must conclude with respect to the aftereffect’s directionality that “the jury is still out.” Moreover, it has been found that numerosity adaptation is bidirectional (i.e., perceived numerosity of dots increases after adapting to small numbers while decreasing after adapting to large numbers; Arrighi, Togoli, & Burr, 2014; Burr & Ross, 2008). Since it has been argued that numerosity perception is based on density coding (Dakin et al., 2011; Morgan et al., 2014; Raphael & Morgan, 2015; Tibber et al., 2012), it is reasonable to conclude that density adaptation is likely to also be bidirectional. However, future studies are needed to clarify this.

Density channels?

A bidirectional SDC is consistent with the idea that density is not represented as a scalar attribute like contrast, but by “channels” that are selective to limited ranges of density. If so, in keeping with explanations of, for example, the tilt illusion (or simultaneous orientation contrast; Blakemore et al., 1970; Clifford, 2014), SDC would arise from inhibition of the channels sensitive to the test by those sensitive to the surround, causing a repulsive shift in the population activity of the test-sensitive channels.

An alternative interpretation might be that the bidirectionality of SDC could have a cognitive origin, i.e., is SDC inferential rather than perceptual? This seems unlikely given that participants were instructed to “ignore” the surround and focus only on the center area.

If there are indeed density channels, as our results suggest, the findings of this study may help to constrain and develop existing models of density coding (Dakin et al., 2011; Durgin, 1999; Kingdom, Hayes, & Field, 2001; Zavitz & Baker, 2014).

Texture density versus numerosity

Although the aim of this communication is not to test directly whether it is density rather than numerosity that mediates SDC in our stimuli, we have assumed from the start that it is density, so some justification for this is necessary. Based on density/numerosity discrimination data, Anobile, Turi, Cicchini, and Burr (2015) argue that for centrally viewed stimuli, densities greater than around 2 dots/deg² are mediated by density not numerosity coding mechanisms. Our central test patches, to which observers directed their judgments, were 6.4 and 12.8 dots/deg², i.e., well within Anobile et al.'s (2015) density-coding range. Moreover, although we found close to a Weber-like decline in precision with density for the with-surround conditions, the without-surround precision showed an approximately square-root decline, in keeping with the density-coding range precisions measured for nonsurrounded stimuli by Anobile, Cicchini, and Burr (2014, 2016).

Our surrounds covered a large range of eccentricities (2.17°–13.04°). According to Anobile et al. (2015), the switch from numerosity to density coding shifts to lower densities with eccentricity, for example to 0.5 dots/deg² for an eccentricity of 15°. We found, however, that surrounds as low as 0.18 and 0.36 dots/deg² ($\times 1/36$ relative surround density conditions), which are within Anobile et al.'s (2015) numerosity range, had an appreciable impact on the perceived density of our test stimuli. This finding appears inconsistent with the idea of independent coding of numerosity and density (Anobile et al., 2014, 2016). Rather, our data are consistent with a common basis for coding density and numerosity (Dakin et al., 2011; Morgan et al., 2014; Raphael & Morgan, 2015; Tibber et al., 2012), with density as the primary visual attribute (Raphael & Morgan, 2015). It nevertheless remains an open question as to whether there are densities sufficiently low to exclusively tap numerosity coding mechanisms in SDC stimuli, in other words whether there is “simultaneous numerosity contrast” (SNC) as well as SDC.

The neurophysiological basis of density coding is not yet clear, but evidence from numerosity studies might provide some hints. Brain imaging studies in both human and monkey show that numerosity information is represented in parietal cortex and lateral prefrontal cortex (Cohen Kadosh, Bien, & Sack, 2012; Dormal, Andres, Dormal, & Pesenti, 2010; Harvey, Klein, Petridou, & Dumoulin, 2013; Nieder, 2012a, 2012b; Piazza & Izard, 2009; Roitman, Brannon, & Platt, 2012; Santens, Roggeman, Fias, & Verguts, 2010; Tudusciuc & Nieder, 2009). Density processing might therefore also occur in these areas, given the close relationship between density and numerosity.

Potential biases

Previous studies have shown that large texture patches are perceived as more dense than small patches of the same density (Bell, Manson, Edwards, & Meso, 2015; Dakin et al., 2011; Raphael, Dillenburger, & Morgan, 2013; Raphael & Morgan, 2015; Tibber et al., 2012). If so we might expect that the tests with surrounds of the same density would be perceived as more dense than tests with no surrounds. The relevant points here are the vertical dashed lines in Figure 3B. However, if anything, the trend is toward observers perceiving the with-surround stimuli as less dense (most points are either at or below the red line), so it would appear that the bias found in previous studies is not manifesting itself here. A likely reason for the lack of a size-based density bias in our stimuli is that observers' judgments were directed to the central test area rather than to the stimulus as a whole.

In generating our stimuli we held constant the degree of regularity across density to prevent dot clusters and blank areas in the more sparse textures, which might have influenced SDC. However, when holding regularity constant, the minimum interdot distance necessarily covaries with density. Could this be a cue? In our pilot studies we did not control for regularity, instead fixing the minimum interdot distance, and found a similar bidirectional SDC. Therefore it seems unlikely that changes in minimum interdot distance with density caused the bidirectional SDC.

Another possible confounding effect related to interdot spacing is perceived distance. It is possible that dense textures appear to lie farther from the viewer than sparse textures due to a form of size constancy that one might term density constancy. As a result, a test of given density surrounded by a sparse (i.e., apparently close) texture might be inferred to be more dense than one surrounded by a dense (i.e., apparently far) texture. However, such an effect is likely to be rather small since dot size, presumably the more significant depth cue, was kept constant, as was also all other depth cues. In addition, participants were asked to focus on the test area, so it seems unlikely that they would make such depth inferences from the interdot distances in the surround.

In our experiments we always presented the variable match stimulus first and then the test stimulus. This design was deemed necessary in order to minimize potential adaptation effects, which might weaken SDC. A potential problem with a fixed and hence known order of presentation is that participants could simply ignore the test interval and base their judgments solely on their memory of the test. However, our use of two test densities, randomly interleaved within a given block, eliminated this possibility.

The role of visual field locus in SDC is not examined in this study, as we always presented test and match stimuli in the center, and the surround stimuli covered a wide range of the visual field. It would be interesting to investigate how location (i.e., eccentricity) affects SDC, and in particular, whether the bidirectionality is preserved in peripheral vision.

Conclusion

Our findings support the idea that there are density-selective channels in the visual system, and that perceived density is in part based on a comparison of these channel responses across space.

Keywords: simultaneous contrast, adaptation, texture, texture density

Acknowledgments

This project was supported by an NSERC (OPG0001978) grant to CB and an NSERC (RGPIN-2016-03915) grant to FK. Thanks also to Frank Durgin for many useful discussions about density coding.

Commercial relationships: none.

Corresponding author: Curtis L. Baker.

Email: curtis.baker@mcgill.ca.

Address: McGill Vision Research, Department of Ophthalmology, McGill University, Montreal, Quebec, Canada.

References

- Anobile, G., Cicchini, G. M., & Burr, D. C. (2014). Separate mechanisms for perception of numerosity and density. *Psychological Science*, *25*(1), 265–270, doi:10.1177/0956797613501520.
- Anobile, G., Cicchini, G. M., & Burr, D. C. (2016). Number as a primary perceptual attribute: A review. *Perception*, *45*(1-2), 5–31, doi:10.1177/0301006615602599.
- Anobile, G., Turi, M., Cicchini, G. M., & Burr, D. C. (2015). Mechanisms for perception of numerosity or texture-density are governed by crowding-like effects. *Journal of Vision*, *15*(5):4, 1–12, doi:10.1167/15.5.4. [PubMed] [Article]
- Arrighi, R., Togoli, I., and Burr, D. C. (2014). A generalized sense of number. *Proceedings of the Royal Society of London B: Biological Sciences*, *281*(1797), 1–7, doi:10.1098/rspb.2014.1791.
- Ban, H., & Yamamoto, H. (2013). A non-device-specific approach to display characterization based on linear, nonlinear, and hybrid search algorithms. *Journal of Vision*, *13*(6):20, 1–26, doi:10.1167/13.6.20. [PubMed] [Article]
- Bell, J., Manson, A., Edwards, M., & Meso, A. I. (2015). Numerosity and density judgments: Biases for area but not for volume. *Journal of Vision*, *15*(2), 18, 1–14, doi:10.1167/15.2.18. [PubMed] [Article]
- Bergen, J. R., & Landy, M. S. (1991). Computational models of visual processing. In M. S. Landy & J. A. Movshon (Eds.), *Computational modeling of visual texture segregation*. (pp. 253–271). Cambridge, MA: MIT Press.
- Blakemore, C., Carpenter, R. H. S., & Georgeson, M. A. (1970). Lateral inhibition between orientation detectors in the human visual system. *Nature*, *228*(5266), 37–39, doi:10.1038/228037a0.
- Brainard, D. H. (1997). The Psychophysics Toolbox. *Spatial Vision*, *10*(4), 433–436, doi:10.1163/156856897X00357.
- Burr, D., & Ross, J. (2008). A visual sense of number. *Current Biology*, *18*(6), 425–428, doi:10.1016/j.cub.2008.02.052.
- Chubb, C., Sperling, G., & Solomon, J. A. (1989). Texture interactions determine perceived contrast. *Proceedings of the National Academy of Sciences, USA*, *86*(23), 9631–9635.
- Clifford, C. W. G. (2014). The tilt illusion: Phenomenology and functional implications. *Vision Research*, *104*, 3–11, doi:10.1016/j.visres.2014.06.009.
- Cohen Kadosh, R., Bien, N., & Sack, A. T. (2012). Automatic and intentional number processing both rely on intact right parietal cortex: A combined fMRI and neuronavigated TMS study. *Frontiers in Human Neuroscience*, *6*, 2, doi:10.3389/fnhum.2012.00002.
- Cutting, J. E., & Millard, R. T. (1984). Three gradients and the perception of flat and curved surfaces. *Journal of Experimental Psychology: General*, *113*(2), 198–216, doi:10.1037/0096-3445.113.2.198.
- Dakin, S. C., Tibber, M., Greenwood, J. A., Kingdom, F. A. A., & Morgan, M. J. (2011). A common perceptual metric for human discrimination of number and density. *Proceedings of the National Academy of Sciences, USA*, *108*(49), 19552–19557, doi:10.1073/pnas.1113195108.
- Dormal, V., Andres, M., Dormal, G., & Pesenti, M. (2010). Mode-dependent and mode-independent

- representations of numerosity in the right intraparietal sulcus. *NeuroImage*, 52(4), 1677–1686, doi:10.1016/j.neuroimage.2010.04.254.
- Durgin, F. H. (1995). Texture density adaptation and the perceived numerosity and distribution of texture. *Journal of Experimental Psychology: Human Perception and Performance*, 21(1), 149–169, doi:10.1037/0096-1523.21.1.149.
- Durgin, F. H. (1996). Visual aftereffect of texture density contingent on color of frame. *Perception & Psychophysics*, 58(2), 207–223, doi:10.3758/bf03211876.
- Durgin, F. H. (1999). A model of texture density encoding. *Investigative Ophthalmology & Visual Science*, 40(12), S200.
- Durgin, F. H. (2001). Texture contrast aftereffects are monocular; texture density aftereffects are binocular. *Vision Research*, 41(20), 2619–2630, doi:10.1016/S0042-6989(01)00121-3.
- Durgin, F. H., & Hammer, J. T. (2001). Visual aftereffects of sequential perception: Dynamic adaptation to changes in texture density and contrast. *Vision Research*, 41(20), 2607–2617, doi:10.1016/S0042-6989(01)00120-1.
- Durgin, F. H., & Huk, A. C. (1997). Texture density aftereffects in the perception of artificial and natural textures. *Vision Research*, 37(23), 3273–3282, doi:10.1016/S0042-6989(97)00126-0.
- Durgin, F. H., & Proffitt, D. R. (1991). Detection of texture density: Evidence from adaptation. Paper presented at the annual meeting of the Psychonomic Society, San Francisco, CA.
- Durgin, F. H., & Proffitt, D. R. (1996). Visual learning in the perception of texture: Simple and contingent aftereffects of texture density. *Spatial Vision*, 9(4), 423–474, doi:10.1163/156856896X00204.
- Efron, B., & Tibshirani, R. J. (1994). *An introduction to the bootstrap*. Boca Raton, FL: CRC Press.
- Field, D. J. (1987). Relations between the statistics of natural images and the response properties of cortical cells. *Journal of the Optical Society of America A*, 4(12), 2379–2394.
- Georgeson, M. A. (1985). The effect of spatial adaptation on perceived contrast. *Spatial Vision*, 1(2), 103–112, doi:10.1163/156856885X00125.
- Harvey, B. M., Klein, B. P., Petridou, N., & Dumoulin, S. O. (2013). Topographic representation of numerosity in the human parietal cortex. *Science*, 341(6150), 1123–1126, doi:10.1126/science.1239052.
- Heinemann, E. G. (1955). Simultaneous brightness induction as a function of inducing-and test-field luminances. *Journal of Experimental Psychology*, 50(2), 89.
- Julesz, B. (1981). Textons, the elements of texture perception, and their interactions. *Nature*, 290(5802), 91–97, doi:10.1038/290091a0.
- Kingdom, F. A. A., Hayes, A., & Field, D. J. (2001). Sensitivity to contrast histogram differences in synthetic wavelet-textures. *Vision Research*, 41(5), 585–598, doi:10.1016/S0042-6989(00)00284-4.
- Kingdom, F. A. A., & Prins, N. (2016). *Psychophysics: A practical introduction, 2nd ed.* London: Academic Press.
- Klein, S., Stromeyer, C. F., & Ganz, L. (1974). The simultaneous spatial frequency shift: A dissociation between the detection and perception of gratings. *Vision Research*, 14(12), 1421–1432, doi:10.1016/0042-6989(74)90017-0.
- Kleiner, M., Brainard, D., and Pelli, D. (2007). *What's new in Psychtoolbox-3?* *Perception*, 36(14), 1.
- Ledgeway, T., Zhan, C., Johnson, A. P., Song, Y., & Baker, C. L., Jr. (2005). The direction-selective contrast response of area 18 neurons is different for first- and second-order motion. *Visual Neuroscience*, 22(1), 87–99, doi:10.1017/s0952523805221120.
- Mackay, D. M. (1973). Lateral interaction between neural channels sensitive to texture density? *Nature*, 245(5421), 159–161, doi:10.1038/245159a0.
- Morgan, M., & MacLeod, D. (2014). Non-orthogonal channels for relative numerosity and contrast detection. *Journal of Vision*, 14(10): 392, doi:10.1167/14.10.392. [Abstract]
- Morgan, M. J., Raphael, S., Tibber, M. S., and Dakin, S. C. (2014). A texture-processing model of the ‘visual sense of number.’ *Proceedings of the Royal Society of London B: Biological Sciences*, 281(1790), doi:10.1098/rspb.2014.1137.
- Nieder, A. (2012a). Coding of abstract quantity by ‘number neurons’ of the primate brain. *Journal of Comparative Physiology A*, 199(1), 1–16, doi:10.1007/s00359-012-0763-9.
- Nieder, A. (2012b). Supramodal numerosity selectivity of neurons in primate prefrontal and posterior parietal cortices. *Proceedings of the National Academy of Sciences*, 109(29), 11860–11865, doi:10.1073/pnas.1204580109.
- Peirce, J. W. (2007). The potential importance of saturating and supersaturating contrast response functions in visual cortex. *Journal of Vision*, 7(6):13, 1–10, doi:10.1167/7.6.13. [PubMed] [Article]
- Pelli, D. G. (1997). The VideoToolbox software for visual psychophysics: Transforming numbers into

- movies. *Spatial Vision*, 10(4), 437–442, doi:10.1163/156856897X00366.
- Piazza, M., & Izard, V. (2009). How humans count: Numerosity and the parietal cortex. *The Neuroscientist*, 15(3), 261–273, doi:10.1177/1073858409333073.
- Portilla, J., & Simoncelli, E. P. (2000). A parametric texture model based on joint statistics of complex wavelet coefficients. *International Journal of Computer Vision*, 40(1), 49–70, doi:10.1023/a:1026553619983.
- Prins, N., & Kingdom, F. A. A. (2009). Palamedes: Matlab routines for analyzing psychophysical data. Retrieved from <http://www.palamedestoolbox.org>
- Raphael, S., Dillenburger, B., & Morgan, M. (2013). Computation of relative numerosity of circular dot textures. *Journal of Vision*, 13(2):17, 1–11, doi:10.1167/13.2.17. [PubMed] [Article]
- Raphael, S., & Morgan, M. J. (2015). The computation of relative numerosity, size and density. *Vision Research*, doi:10.1016/j.visres.2014.12.022.
- Roberts, B., Harris, M. G., & Yates, T. A. (2005). The roles of inducer size and distance in the Ebbinghaus Illusion (Titchener circles). *Perception*, 34(7), 847–856, doi:10.1068/p5273.
- Roitman, J. D., Brannon, E. M., & Platt, M. L. (2012). Representation of numerosity in posterior parietal cortex. *Frontiers in Integrative Neuroscience*, 6, 25, doi:10.3389/fnint.2012.00025.
- Santens, S., Roggeman, C., Fias, W., & Verguts, T. (2010). Number processing pathways in human parietal cortex. *Cerebral Cortex*, 20(1), 77–88, doi:10.1093/cercor/bhp080.
- Tibber, M. S., Greenwood, J. A., & Dakin, S. C. (2012). Number and density discrimination rely on a common metric: Similar psychophysical effects of size, contrast, and divided attention. *Journal of Vision*, 12(6):8, 1–19, doi:10.1167/12.6.8. [PubMed] [Article]
- Todd, J. T., & Thaler, L. (2010). The perception of 3D shape from texture based on directional width gradients. *Journal of Vision*, 10(5):17, 1–13, doi:10.1167/10.5.17. [PubMed] [Article]
- Tudusciuc, O., & Nieder, A. (2009). Contributions of primate prefrontal and posterior parietal cortices to length and numerosity representation. *Journal of Neurophysiology*, 101(6), 2984–2994, doi:10.1152/jn.90713.2008.
- Zavitz, E., & Baker, C. L. (2013). Texture sparseness, but not local phase structure, impairs second-order segmentation. *Vision Research*, 91, 45–55, doi:10.1016/j.visres.2013.07.018.
- Zavitz, E., & Baker, C. L. (2014). Higher order image structure enables boundary segmentation In the absence of luminance or contrast cues. *Journal of Vision*, 14(4):14, 1–14, doi:10.1167/14.4.14. [PubMed] [Article]